Beamforming OLEDs for sensing applications employing a nanostructured fluorescent waveguide layer

Buhl, Janek, Lüder, Hannes, Nolte, Tim, Sbrisny, Fynn Ole, Gerken, Martina

Janek Buhl, Hannes Lüder, Tim Nolte, Fynn Ole Sbrisny, Martina Gerken, "Beamforming OLEDs for sensing applications employing a nanostructured fluorescent waveguide layer," Proc. SPIE 11998, Organic Photonic Materials and Devices XXIV, 1199802 (7 March 2022); doi: 10.1117/12.2608647

SPIE.

Event: SPIE OPTO, 2022, San Francisco, California, United States

Beamforming OLEDs for sensing applications employing a nanostructured fluorescent waveguide layer

Janek Buhl*[a], Hannes Lüder[a], Tim Nolte[a], Fynn Ole Sbrisny[a], Martina Gerken[a]
[a]Kiel University, Faculty of Engineering, Kaiserstr. 2, 24143 Kiel, Germany

ABSTRACT

Organic light-emitting diodes (OLEDs) hold great promise as light sources for miniaturized and monolithically integrated optical sensors. Their unique properties and flexible processing methods enable the realization of disposable or recyclable lab-on-a-chip systems by combining multiple light sources and detector units on a single substrate. One of the main challenges in these systems is tailoring of light emission characteristics in order to illuminate specific sensing spots without the use of external optical components. Since OLEDs typically exhibit wide-angle light emission across the device surface, we propose the implementation of a nanostructured fluorescent waveguide. This layer acts as a color conversion filter by absorbing OLED light while providing narrow-angle emission of fluorescent light propagating in the waveguide. The appropriate choice of OLED emission color, fluorescent dye and nanostructure design allows for tailoring of the emission wavelength and beam characteristics. We investigate the impact of various fabrication parameters such as the layer thickness and fluorophore concentration on the color conversion efficiency as well as the directionality of the outcoupled fluorescent light. While high absorption of the OLED excitation light is beneficial in order to suppress wide-angle background emission, we show that high fluorophore content may lead to fluorescence quenching and reabsorption of fluorescent light inside the waveguide impairing resonant outcoupling effects.

Keywords: organic light-emitting diode, directional light emission, beamforming, nanostructured fluorescent waveguide, resonant light-outcoupling, optical sensing, lab on a chip

1. INTRODUCTION

Optical sensor systems are widely utilized in a range of different applications, such as health monitoring, diagnostics or agricultural sensing. They typically comprise one or more light sources, an optical path consisting of multiple components to guide the light and one or more detector units. Due to the oftentimes complex optical setups most of the systems employed for quantitative analysis are large, expensive and only available in dedicated laboratories. Lab-on-a-chip (LOC) devices, in contrast, offer cost- and time-efficient point-of-need analysis by combining microfluidic sample chambers with miniaturized data acquisition and readout systems.[1] Organic optoelectronics, i.e. organic light-emitting diodes (OLEDs) and organic photodetectors (OPDs), are well suited for these purposes because they can be realized in almost arbitrary shapes and sizes and on flexible plastic substrates in order to match specific application requirements. Additionally, they can potentially be fabricated using low-cost, high-throughput printing techniques.[2] Miniaturized OLED-OPD-sensing units have been demonstrated for various applications, such as pulse oximetry,[3,4] oxygen and pH sensing,[5] and fluorescence detection.[6] They usually consist of two individual substrates holding the light source and the detector, which are either arranged separately or laminated on top of each other to obtain a joined device. Another highly promising approach is based on a monolithically integrated design where multiple OLED light sources and organic photodetectors are processed on a common single substrate.[7] In this case, the light source and the photodetector are placed side by side preventing direct illumination of the detection unit and making the design suitable for fluorescence measurements.

Since the individual optoelectronic devices are small in size, precise control over the OLED emission characteristics is required to obtain sufficient signal intensity. In order to maximize signal intensity, the sensing spot should be as close as possible to the detection unit, i.e. directly above the OPD. In conventional OLEDs, however, light intensity decreases at higher angles due to the radiation pattern approximately following Lambert's cosine law.[8] In the proposed side-by-side configuration shown in Figure 1a, only a small fraction of the available excitation light would consequently reach the sensing spot, limiting the sensitivity of the entire system.

*jabu@tf.uni-kiel.de; +49 431 880-6259; fax +49 431 880-6253; www.isp.tf.uni-kiel.de

Organic Photonic Materials and Devices XXIV, edited by William M. Shensky III, Ileana Rau, Okihiro Sugihara,
Proc. of SPIE Vol. 11998, 1199802 · © 2022 SPIE · 0277-786X · doi: 10.1117/12.2608647

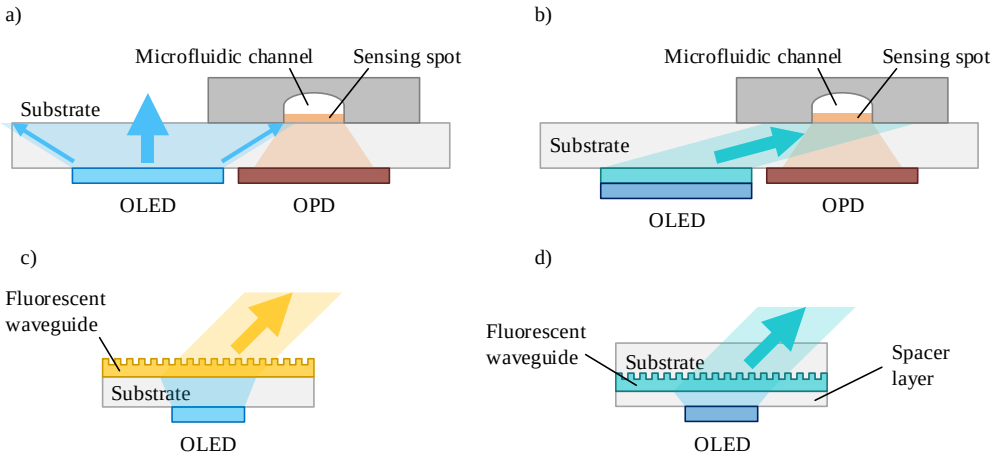

Figure 1. Schematic representation of the side-by-side configuration featuring an OLED and an OPD fabricated on a single substrate (a). The sensing spot inside the microfluidic sample chamber is located directly above the detector. Directional illumination can be achieved by combining a conventional OLED with a nano-patterned fluorescent waveguide (b). In the device structure investigated in this work, the waveguide layer is deposited on the backside of the OLED substrate to allow for isolated optical characterization (c). For system integration, the waveguide layer may be placed on the OLED side of the substrate, separated by a spacer layer (d).

Tailoring of the optical path by use of external optical components such as lenses, mirrors and apertures is not easily feasible as it introduces novel challenges with regard to further miniaturization, system integration and additional alignment concerns in the LOC system. In contrast, system sensitivity may be increased significantly by employing beamforming OLEDs with directional light emission towards specific sensing spots. A simple way to obtain directional light emission from OLEDs is the usage of a periodically nano-patterned optical waveguide, resulting in resonant out-coupling of quasi-guided modes[9]. The layer stack forming the OLED itself is commonly used as the waveguide by integrating a periodic nanopattern into the bottom electrode or the organic layers.[10-12] Directional outcoupling of substrate modes is also achievable by placing a diffractive optical element adjacent to the OLED.[13] Here, we demonstrate the application of a dedicated fluorescent waveguide layer in conjunction with a conventional OLED (see Figure 1b). By spatially separating the waveguide from the semiconductor stack, high quality factors are obtainable, leading to sharp resonant emission peaks. The appropriate choice of OLED emission spectrum, fluorescent compound and nanostructure design allows for tailoring of emission wavelength and beam characteristics according to application requirements.

2. DEVICE STRUCTURE AND MATERIALS

The structure of the proposed device is depicted schematically in Figure 1c. The periodically nano-patterned fluorescent waveguide is situated on the backside of the OLED carrier substrate to facilitate the separate optical investigations reported in this work. For final system integration, placement of the waveguide layer in between the substrate and the OLED stack may be favorable allowing for the attachment of a microfluidic sample chamber on the device backside (see Figure 1d). As the waveguide comprises a fluorescent compound, it acts as a color conversion layer (CCL), similar to numerous reports of OLEDs featuring CCLs in order to modify the emission color or obtain white emission.[14,15] In the proposed device structure, wide-angle OLED light is absorbed in the fluorescent layer while fluorescent light is reemitted into the waveguide. The light propagating in the waveguide is then resonantly coupled out of the device structure due to Bragg scattering.[16] The outcoupling angle ϑ for each wavelength λ_0 depends on the period length of the nanopattern Λ as well as the effective refractive index n_{eff} and can be estimated according to Equation 1.

$$\vartheta = \pm \arcsin\left(n_{\mathrm{eff}} - \lambda_0/\Lambda\right) \tag{1}$$

The objective of the proposed device structure is directional light emission at a specific wavelength from an arbitrary emission surface defined by the OLED shape while minimizing background emission, i.e. direct transmission of OLED

light through the waveguide and non-directional fluorescence. As device performance is affected by several optical characteristics, we will briefly discuss the most important parameters.

Absorption of OLED excitation light inside the waveguide plays a crucial role for both color conversion as well as suppression of background emission. While high absorption of the OLED light is required, absorption in the spectral range of the fluorescent emission deteriorates light propagation properties of the waveguide, impairing resonance effects. Apart from exhibiting high quantum yield, the fluorescent compound should therefore have minimal overlap of the absorption and emission spectra (i.e. a reasonably large Stokes shift) to avoid reabsorption of the fluorescent light inside the waveguide. Additionally, quenching effects occurring in the solid layer may reduce fluorescence intensity. Finally, the total thickness determines the number of optical modes that can propagate in the waveguide. A high number of optical modes results in multiple resonant outcoupling peaks at a single angle. While this effect may decrease specificity of the light source, it also offers additional application potential. It should, however, be noted, that the absorption inside the waveguide layer cannot simply be enhanced by increasing the layer thickness without affecting its optical properties.

The spectral position of the resonance effects mainly depends on the nanopattern periodicity and the refractive index of the waveguide. Here, we propose two slightly different approaches to obtain a fluorescent high-index layer serving as the waveguide, which can be deposited using a simple solution process. Fluorescent polymers, such as poly(*p*-phenylene vinylene) (PPV) and associated copolymers, often exhibit intrinsically high refractive indices.[17,18] An appropriate polymer layer can thus be employed as a single-material fluorescent waveguide. While this facilitates device fabrication, optical properties such as absorption and fluorescence intensity depend exclusively on the layer thickness. An alternative approach is based on the utilization of a small molecule fluorophore doped into a transparent high-index polymer forming the waveguide. In this case, optical parameters can be adjusted independently by selecting the optimal fluorophore concentration for a given layer thickness. This work is focused on three different waveguide compositions: We investigate the well-known and widely-used fluorescent polymers Poly(9,9-dioctylfluorene-alt-benzothiadiazole) (F8BT, $\lambda_{max} \approx 550$ nm) and PDY-132 (Super Yellow, $\lambda_{max} \approx 570$ nm) and the laser dye 4-(Dicyanomethylene)-2-methyl-6-(4-dimethylaminostyryl)-4*H*-pyran (DCM, $\lambda_{max} \approx 650$ nm) doped in polyvinylcarbazole (PVK). Figure 2 shows normalized absorption and photoluminescence (PL) emission spectra of the different waveguide compositions coated on a glass substrate. All three fluorophores exhibit strong absorption between 450 nm and 500 nm, high fluorescence intensity as well as relatively large Stokes shifts, making them suitable candidates for the intended application.

Fabrication parameters have to be chosen carefully for each configuration because material properties may differ significantly. Here, we investigate the impact of layer thickness and fluorophore concentration on the color conversion and directionality of the emitted fluorescent light.

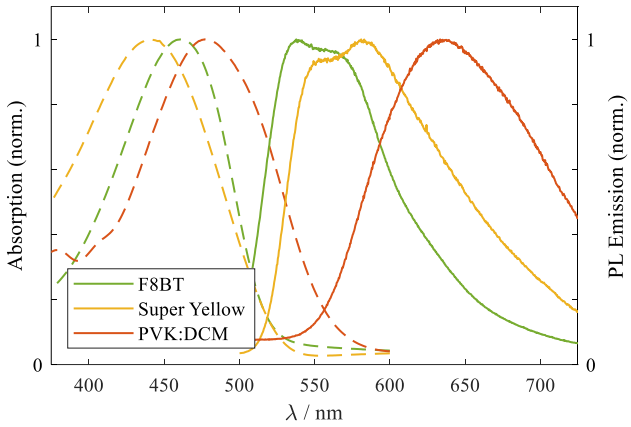

Figure 2. Normalized absorption spectra (dashed lines) and photoluminescence (PL) emission spectra (solid lines) of the three waveguide compositions under investigation.

3. EXPERIMENTAL

All samples used in this work were prepared on soda-lime glass substrates with a size of 25 × 25 mm². Nanopatterns were fabricated by UV nanoimprint lithography as detailed in [19]. Commercially available glass templates holding a one-dimensional periodic grating with a period length of 372 nm were used to replicate the nanopattern in the UV-curable imprint resist Ammonil MMS4 (Amo GmbH). Subsequently, fluorophore solutions were spin-coated onto the cured imprint resist at 1400 rpm to obtain homogenously coated nano-patterned fluorescent layers. Solutions were prepared by dissolving different concentrations of F8BT ($M_n \leq 25000$, Merck), PDY-132 (Merck) and PVK:DCM (Merck) in either toluene (F8BT and PDY-132) or a 1:1 mixture of toluene and *o*-dichlorobeneze (PVK:DCM) and stirring over night at 55 °C. The resulting layer thickness was measured with a profilometer (Ambios). Optical absorption measurements were performed using a UV-Vis spectrophotometer (PerkinElmer). An in-house built goniophotometer setup comprising an automatic rotational stage (Newport) and an imaging spectrometer (Oxford Instruments) was employed to record angle-resolved fluorescence spectra.

Fabrication of bottom-emitting OLEDs was carried out on glass substrates coated with indium-doped tin oxide (ITO) by thermal evaporation. The emission material bis[2-(4,6-difluorophenyl)pyridinato-C2,N](picolinato)iridium(III) (FIrpic) (Luminescence Technology Corp.) was used in the following layer stack to obtain a blue emission color: ITO (140 nm) | MoO_3 (5 nm) | 1,1-bis[(di-4-tolylamino)phenyl]cyclohexane (TAPC) (35 nm) | tris(4-carbazoyl-9-ylphenyl)amine (TCTA):8 % FIrpic (20 nm) | 2,2',2"-(1,3,5-benzinetriyl)-tris(1-phenyl-1-H-benzimidazole) (TPBi) (50 nm) | LiF (1 nm) | Al (200 nm). Active emission area size was 5 × 5 mm². The completed OLED devices were encapsulated in a nitrogen-filled glovebox to allow for optical measurements in air. After device fabrication, the UV nanoimprint process and fluorophore coating were performed on the substrate's backside.

4. RESULTS

We fabricated non-patterned fluorescent layers by spin-coating solutions with different fluorophore concentrations onto planar glass substrates to determine optical properties of the corresponding waveguides. Figure 3 shows absolute absorption and photoluminescence emission spectra of the resulting layers comprising F8BT, Super Yellow and PVK:DCM at various thicknesses. Color conversion efficiency can be evaluated qualitatively by comparison of the absorption and emission intensity at different thicknesses. As expected, optical absorption is enhanced with increasing layer thickness and fluorophore content for all three waveguide compositions. Fluorescence intensity, however, does not exhibit the same dependency, suggesting differences in color conversion efficiency. In case of the Super Yellow waveguide, PL emission decreases slightly at very high layer thickness. This effect may be caused by reabsorption of fluorescent light inside the waveguide due to the slight overlap of the absorption and emission spectrum. Comparison of two PVK:DCM waveguides featuring approximately the same layer thickness (632 nm and 616 nm) but different DCM content (10 wt% and 14 wt%) shows that the layer with higher DCM content exhibits higher absorption but lower PL emission. This decrease in color conversion efficiency may be attributed to quenching effects arising at high fluorophore concentrations.

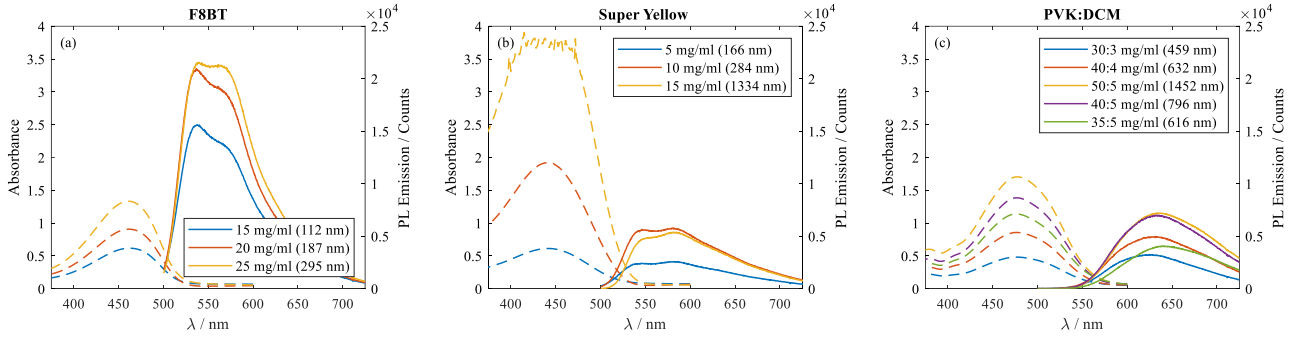

Figure 3. Absolute absorption spectra (dashed lines) and photoluminescence (PL) emission spectra (solid lines) of the three waveguide compositions under investigation. Absorption increases invariably with increasing layer thickness and fluorophore concentration while PL emission partly decreases, indicating differences in quantum efficiency due to fluorescence quenching. All PL spectra have been measured using exactly the same excitation conditions.

In addition to the non-directional emission intensity, quenching or reabsorption of fluorescent light may also affect resonance effects. We chose the PVK:DCM waveguide to study the impact of fluorophore content on resonant light outcoupling because it allows for variation of the fluorophore (DCM) content without changing the concentration of the high-index material (PVK). Figure 4 shows PL emission spectra of two waveguide layers with fluorophore contents of 10 wt% and 20 wt% recorded at different angles with respect to the surface normal. Resonant outcoupling peaks are clearly observable at different wavelengths depending on the viewing angle. At lower fluorophore content, however, peak intensity is much higher, resulting in higher emission directionality. At higher fluorophore content, the spectral shape of the outcoupling peaks is broadened considerably, limiting the maximum outcoupling intensity. The decrease in quality factor can likely be attributed to the high fluorophore content introducing additional absorption. Residual transmission of the excitation light around 450 nm is present in all graphs with the intensity of the excitation peak being higher at lower fluorophore content due to differences in absorption.

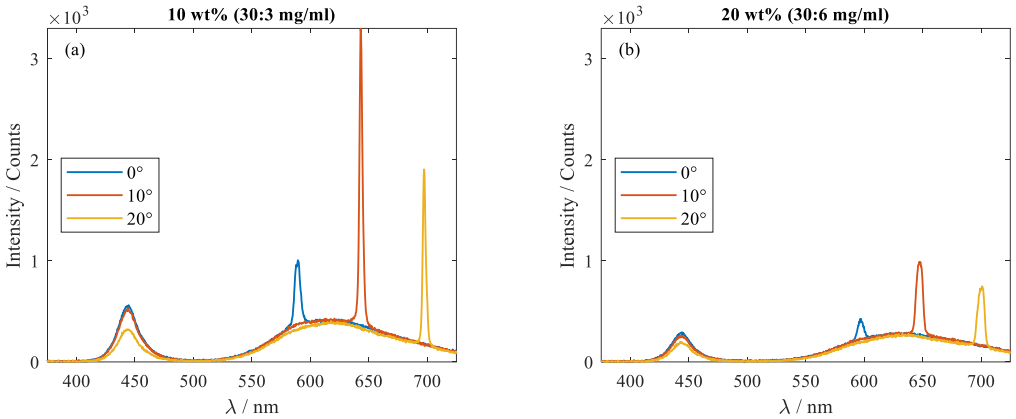

Figure 4. Absolute photoluminescence (PL) emission spectra of two nano-patterned PVK:DCM waveguide layers comprising a fluorophore content of 10 wt% (a) and 20 wt% (b) at different viewing angles. Comparison of the peak intensity and shape suggests that high fluorophore content adversely affects resonant outcoupling.

Taking into consideration the differences in color conversion efficiency as well as a maximum layer thickness of around 700 nm (to not allow for a multitude of resonant optical modes in the relevant spectral range), we fabricated nano-patterned fluorescent waveguides on glass substrates utilizing the following fluorophore concentrations: 25 mg/ml F8BT, 10 mg/ml Super Yellow and 40:4 mg/ml PVK:DCM.

Subsequently, we investigated resonant light outcoupling from the fluorescent waveguides by measuring the angular dependence of the fluorescent light under external excitation at 450 nm. Angle-resolved photoluminescence spectra of the three waveguide compositions are depicted in Figure 5. All spectra include sharp resonant peaks following a characteristic “X-shape” in accordance to Equation 1. The waveguides comprising F8BT and Super Yellow show high intensity of resonant emission compared to the fluorescent background emission and strong suppression of the excitation light. Additionally, both single-material waveguides feature a clearly observable optical mode as well as a second less pronounced mode at lower wavelengths. In contrast, the PVK:DCM waveguide exhibits only a single resonant peak at nearly all angles due to the spectral position of the resonance. Emission directionality, however, is slightly decreased due to higher intensity of non-directional fluorescent emission.

Figure 6 shows emission spectra of a final OLED device coated with a PVK:DCM waveguide. The uncoated reference device has its emission maximum between at 495 nm exhibiting no angular dependence. Although resonance peaks are clearly recognizable between 600 nm and 725 nm, the emission maximum of the coated device is at 550 nm. The comparatively low intensity of the resonance effects may be attributed to the spectral shape of the FIrpic OLED, which exhibits a very broad emission spectrum, unlike the external light source used for the PL measurements shown before. Since the fluorophore’s absorption curve declines steeply above 520 nm, the majority of the OLED excitation light is transmitted through the waveguide in this spectral range. The resulting non-directional background emission consequentially decreases emission directionality of the device.

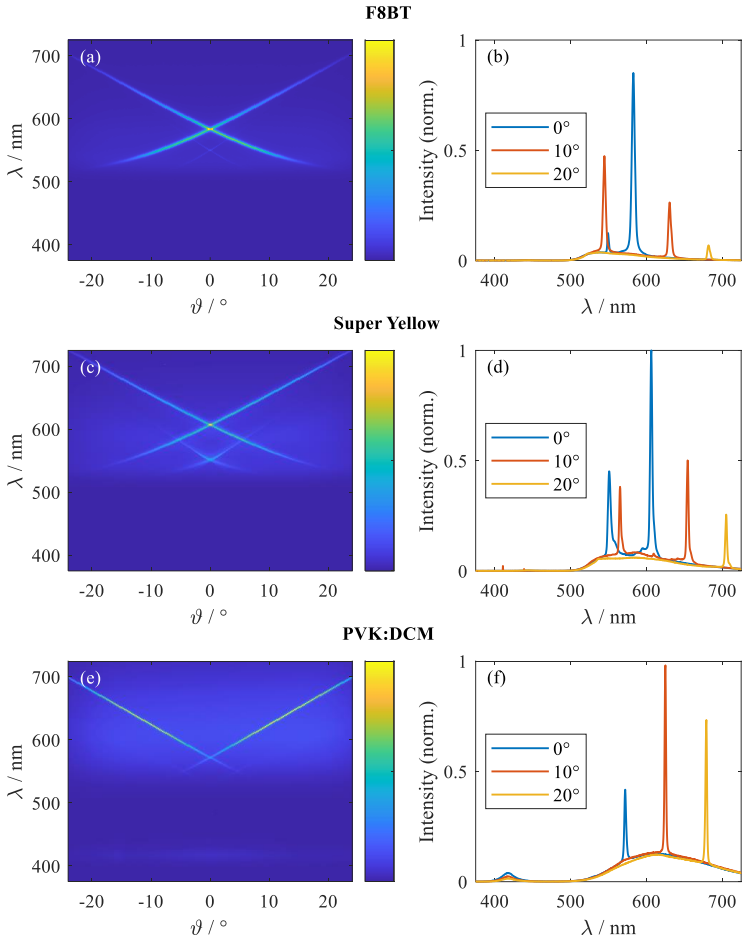

Figure 5. Angle-resolved photoluminescence spectra and spectral cuts at select angles of nano-patterned fluorescent waveguide layers. Although sharp resonant peaks are observable for all waveguide compositions, F8BT and Super Yellow waveguides exhibit higher directionality of light emission. Signal intensity below 450 nm corresponds to residual transmission of scattered excitation light.

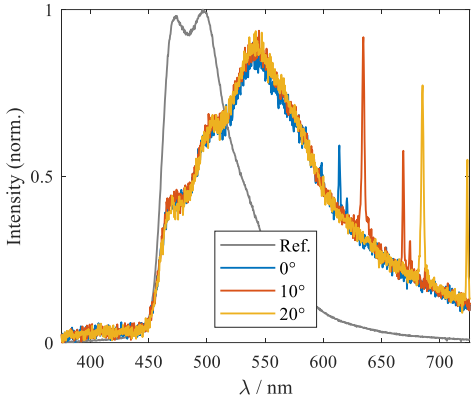

Figure 6. Emission spectrum of an OLED device coated with a nano-patterned fluorescent waveguide layer comprising PVK:DCM (40:4 mg/ml) at different viewing angles. Resonant outcoupling effects can be observed, but light directionality is low due to background transmission of the OLED light. The grey line corresponds to the emission spectrum of an uncoated reference OLED.

5. CONCLUSIONS

We demonstrate the application of nano-patterned fluorescent waveguide layers to obtain directional emission from OLED devices. We propose three different waveguide compositions, investigating the impact of layer thickness and fluorophore concentration on the absorption of the non-directional excitation light and fluorescence intensity for each composition. While background suppression increases at high fluorophore content, we show that quenching effects and reabsorption of fluorescent light may reduce resonant outcoupling. Using carefully chosen fabrication parameters, high resonant emission peaks are obtained at different viewing angles and wavelengths by optical excitation. Additionally, we show single-substrate integration of a blue OLED and a PVK:DCM waveguide yielding resonant outcoupling of fluorescent light under OLED illumination. Since emission directionality is limited by background transmission of the excitation light, we expect significantly higher device performance when combining the fluorescent waveguide with a narrow-band deep-blue OLED. In conclusion, we believe our results to be an important step towards the realization of beamforming OLEDs, which may be employed in a range of different sensing applications.

ACKNOWLEDGMENTS

This project has received funding from the European Research Council (ERC) under the European Union's Horizon 2020 research and innovation programme (grant agreement No 899861).

REFERENCES

[1] Luka, G., Ahmadi, A., Najjaran, H., Alocilja, E., Derosa, M., Wolthers, K., Malki, A., Aziz, H., Althani, A. and Hoorfar, M., "Microfluidics Integrated Biosensors: A Leading Technology towards Lab-on-a-Chip and Sensing Applications," Sensors **15**(12), 30011–30031 (2015).

[2] Abbel, R., De Vries, I., Langen, A., Kirchner, G., T'Mannetje, H., Gorter, H., Wilson, J. and Groen, P., "Toward high volume solution based roll-to-roll processing of OLEDs," J. Mater. Res. **32**(12), 2219–2229 (2017).

[3] Yokota, T., Zalar, P., Kaltenbrunner, M., Jinno, H., Matsuhisa, N., Kitanosako, H., Tachibana, Y., Yukita, W., Koizumi, M. and Someya, T., "Ultraflexible organic photonic skin," Sci. Adv. **2**(4) (2016).

[4] Khan, Y., Han, D., Ting, J., Ahmed, M., Nagisetty, R. and Arias, A. C., "Organic multi-channel optoelectronic sensors for wearable health monitoring," IEEE Access **7**, 128114–128124 (2019).

[5] Liu, R., Xiao, T., Cui, W., Shinar, J. and Shinar, R., "Multiple approaches for enhancing all-organic electronics photoluminescent sensors: Simultaneous oxygen and pH monitoring," Anal. Chim. Acta **778**, 70–78 (2013).

[6] Lefèvre, F., Juneau, P. and Izquierdo, R., "Integration of fluorescence sensors using organic optoelectronic components for microfluidic platform," Sensors Actuators B Chem. **221**, 1314–1320 (2015).

[7] Titov, I., Kopke, M., Schneidewind, N. C., Buhl, J., Murat, Y. and Gerken, M., "OLED-OPD Matrix for Sensing on a Single Flexible Substrate," IEEE Sens. J. **20**(14), 7540–7547 (2020).

[8] Kim, J. S., Ho, P. K. H., Greenham, N. C. and Friend, R. H., "Electroluminescence emission pattern of organic light-emitting diodes: Implications for device efficiency calculations," J. Appl. Phys. **88**(2), 1073 (2000).

[9] Lüder, H. and Gerken, M., "FDTD modelling of nanostructured OLEDs: analysis of simulation parameters for accurate radiation patterns," Opt. Quantum Electron. **51**(5), 1–20 (2019).

[10] Lupton, J. M., Matterson, B. J., Samuel, I. D. W., Jory, M. J. and Barnes, W. L., "Bragg scattering from periodically microstructured light emitting diodes," Appl. Phys. Lett. **77**(21), 3340 (2000).

[11] Fujita, M., Ishihara, K., Ueno, T., Asano, T., Noda, S., Ohata, H., Tsuji, T., Nakada, H. and Shimoji, N., "Optical and electrical characteristics of organic light-emitting diodes with two-dimensional photonic crystals in organic/electrode layers," Japanese J. Appl. Physics **44**(6 A), 3669–3677 (2005).

[12] Zhang, S., Turnbull, G. A. and Samuel, I. D. W., "Enhancing the emission directionality of organic light-emitting diodes by using photonic microstructures," Appl. Phys. Lett. **103**(21), 213302 (2013).

[13] Zhang, S., Turnbull, G. A., W Samuel, I. D., Zhang, S., Turnbull, G. A. and W Samuel, I. D., "Highly Directional Emission and Beam Steering from Organic Light-Emitting Diodes with a Substrate Diffractive Optical Element," Adv. Opt. Mater. **2**(4), 343–347 (2014).
[14] Hu, Z., Yin, Y., Ali, M. U., Peng, W., Zhang, S., Li, D., Zou, T., Li, Y., Jiao, S., Chen, S. J., Lee, C. Y., Meng, H. and Zhou, H., "Inkjet printed uniform quantum dots as color conversion layers for full-color OLED displays," Nanoscale **12**(3), 2103–2110 (2020).
[15] Ho, Y.-H., Huang, D.-W., Chang, Y.-T., Ye, Y.-H., Chu, C.-W., Tian, W.-C., Chen, C.-T. and Wei, P.-K., "Improve efficiency of white organic light-emitting diodes by using nanosphere arrays in color conversion layers," Opt. Express **20**(3), 3005–3014 (2012).
[16] Kluge, C., Rädler, M., Pradana, A., Bremer, M., Jakobs, P.-J., Barié, N., Guttmann, M. and Gerken, M., "Extraction of guided modes from organic emission layers by compound binary gratings," Opt. Lett. **37**(13), 2646–2648 (2012).
[17] Smirnov, J. R. C., Zhang, Q., Wannemacher, R., Wu, L., Casado, S., Xia, R., Rodriguez, I. and Cabanillas-González, J., "Flexible all-polymer waveguide for low threshold amplified spontaneous emission," Sci. Reports **6**(1), 1–6 (2016).
[18] Lim, H. S., Lee, J. H., Jeong, H. Y. and Cho, S. O., "Lasing from MEH-PPV with a refractive index tunable by electron irradiation," Opt. Express **29**(13), 19945–19954 (2021).
[19] Jahns, S., Bräu, M., Meyer, B.-O., Karrock, T., Gutekunst, S. B., Blohm, L., Selhuber-Unkel, C., Buhmann, R., Nazirizadeh, Y. and Gerken, M., "Handheld imaging photonic crystal biosensor for multiplexed, label-free protein detection.," Biomed. Opt. Express **6**(10), 3724–3736 (2015).